coatings

MDPI

Article

Dispersion of Carbon Nanotubes Improved by Ball Milling to Prepare Functional Epoxy Nanocomposites

Ziqi Gao [1], Quanjiabao Han [2], Jianbang Liu [1,*], Kangbo Zhao [2], Yin Yu [2], Yuanyuan Feng [1] and Sensen Han [3,4,*]

[1] College of Civil Aviation, Shenyang Aerospace University, Shenyang 110136, China
[2] College of Aerospace Engineering, Shenyang Aerospace University, Shenyang 110136, China
[3] School of Materials Science and Engineering, University of Science and Technology of China, Shenyang 110016, China
[4] Shi-Changxu Innovation Center for Advanced Materials, Institute of Metal Research, Chinese Academy of Sciences, Shenyang 110016, China
* Correspondence: liu.jianbang@sau.edu.cn (J.L.); sauhansen@163.com (S.H.)

Abstract: There has been an increase in interest in developing functional polymer composites based on green chemistry principles. The purpose of this study was to investigate the preparation of functional epoxy/carbon nanotube nanocomposites using ball milling methods. In contrast to mechanical mixing, ball milling promoted good dispersion of CNTs within the epoxy matrix, thereby improving their mechanical properties and electrical conductivity. In epoxy nanocomposites with ball milling, Young's modulus and tensile strength were increased by 653% and 150%, respectively, when CNT loading was 1.0 vol%. Additionally, the ball milling of CNTs improves their dispersion, resulting in a low percolation threshold at 0.67 vol%. The epoxy/CNT film sensor that was produced using the ball milling approach not only exhibited high reliability and sensitivity to mechanical strains and impact loads, but also possessed the ability to self-detect damage, such as cracks, and accurately locate them. This study marks a notable milestone in the advancement of functional epoxy/CNT composites through the ball milling approach.

Keywords: epoxy; carbon nanotube; dispersion; ball milling

Citation: Gao, Z.; Han, Q.; Liu, J.; Zhao, K.; Yu, Y.; Feng, Y.; Han, S. Dispersion of Carbon Nanotubes Improved by Ball Milling to Prepare Functional Epoxy Nanocomposites. *Coatings* **2023**, *13*, 649. https://doi.org/10.3390/coatings13030649

Academic Editor: Csaba Balázsi

Received: 28 February 2023
Revised: 16 March 2023
Accepted: 17 March 2023
Published: 20 March 2023

1. Introduction

Epoxy resins, a crucial type of thermosetting polymers [1], are becoming increasingly popular for various applications such as in-surface coating [2], painting, and laminates, due to their desirable properties, including high strength, low creep, minimal curing shrinkage, excellent chemical and corrosion resistance, good workability, cost-effectiveness, and compatibility with a wide range of substrates [3–5]. Epoxy resin is an intrinsically non-conductive material with a conductivity of approximately 10^{-13} S/cm. However, there is a significant need for electrically conductive epoxy composites in the aerospace and electronics industries [6], primarily materials that are electrically anti-static. To meet this demand, conductive nanofillers such as metal-based particles and carbon-based materials are added to the epoxy matrix to improve its electrical conductivity. Self-sensing refers to the ability of a structural material to sense its own condition, such as strain, damage, and temperature. Structural materials possess intrinsic properties that can be leveraged to achieve self-sensing. Accurate detection and measurement of damage in structural components are critical, as they provide valuable information for maintenance and re-pair, particularly in the field of civil engineering [7].

With the increasing demand for flexible and multifunctional materials that possess enhanced mechanical and electrical properties, especially for specific applications such as modern electronics, aerospace, and automotive structures [8–11], the development of advanced epoxy composites has received significant attention. However, the poor mechanical

and functional properties of epoxy resins significantly limit their wide-ranging applications. To address this challenge, the incorporation of nanofillers into epoxy resins through nanocomposite technology has been shown to be a promising approach to improving their functional, electrical, and structural properties [12–15]. The enhanced properties of these composites could lead to their potential application in signal sensing, depending on their attained features [16–18].

A variety of conductive materials, such as gold nanoparticles, gold and silver nanowires [19], graphene [20–22], and carbon nanotubes (CNTs) [23], were investigated for the development of multifunctional polymer-based composite films. Due to their high density, metal-based sensors are usually heavy and have poor stretchability. When compared to metallic nanoparticles, polymeric composite films and sensors developed using carbon nanotubes and graphene are light, flexible, and stretchable.

CNTs are one-dimensional (1D) tubes with exceptional mechanical properties and aspect ratios ranging from 30 to thousands. CNTs and CNT-based derivatives [24–26] have seen a significant increase in interest in recent years due to their high chemical stability, unique morphology, and electronic and mechanical properties. Adding CNTs or CNT derivatives to polymers at extremely low loading enhances their electrical, thermal, and mechanical properties [27]. Several studies have investigated the structure-property relations of polymer/graphene and CNT nanocomposites. The dispersion and interfacial adhesion of carbon-based nanomaterials within an epoxy matrix are critical factors affecting the performance enhancement of epoxy nanocomposites [28–32]. In addition, it is important to note that polymer properties, nanofiller conductivity, structural characteristics, and dispersion quality are key factors affecting composite-based sensor performance.

For compounding nanofillers with epoxy, there are several traditional methods, including in-situ polymerization, solution mixing, and melt compounding, that cause pollution to the environment and do not adhere to sustainable development and green chemistry concepts. In the present study, a green, cost-effective method is presented for the manufacture of high-performance epoxy nanocomposites containing homogeneously dispersed nanofillers. Low-cost, environmentally friendly, large production scale, and versatile ball mills have been widely used in industrial production for many years. A growing focus has been placed on eco-friendly polymer composite synthesis in recent years. For example, Deng et al. describes how wet ball milling was used to uniformly disperse and reduce the size of clusters of halloysite particles in an epoxy matrix [33], whereas planetary mechanical milling was used to fabricate a UV-curable epoxy/OMMT nanocomposite [34].

Using ball-milled carbon nanotubes (CNTs) may improve their dispersion within the epoxy matrix, resulting in enhanced mechanical and functional properties. In this study, we examine the morphology, mechanical properties, and functional properties of epoxy nanocomposites. Electrical and thermal conductivity, as well as self-sensing properties, have been demonstrated in epoxy/CNT nanocomposites. Ball milling is a low-cost, eco-friendly, and practical method for dispersing CNTs and producing high-performance epoxy nanocomposites, according to the study.

2. Experiment

2.1. Materials

Chengdu Organic Chemicals Pty Ltd., Chinese Academy of Sciences, provided multiwalled CNTs with diameters ranging from 8–15 nanometers, lengths of approximately 50 μm, and 98% purity with intrinsic electrical conductivity > 100 S/cm. We purchased 184–200 g of diglycidyl ether of bisphenol A (E-51) from Nantong Xingchen Synthetic Material. Huntsman, China supplied Hardener, Jeffaimne D 2000 (J2000). The other chemicals used were analytical grade and were used as received.

2.2. Preparation

Unwound carbon nanotubes: The unwinding of carbon nanotubes (CNTs) is based on wall breaker crushing and ball milling combined, as shown in Figure 1. Briefly, 0.1 g

of multi-walled CNTs were dispersed in 200 mL of deionized water in a wall breaker for 30 min, with a 1 min break every 1 min, to avoid overheating. After blending, the 100 mL CNTs suspension was poured into a ball mill jar containing zirconia balls 4 mm in diameter. A rotation speed of 400 rpm was used and the grinding process was programmed to run for 30 h, with a 10 min break every 30 min to avoid overheating. The mixture was separated by centrifugation, washed with deionized water, and freeze-dried.

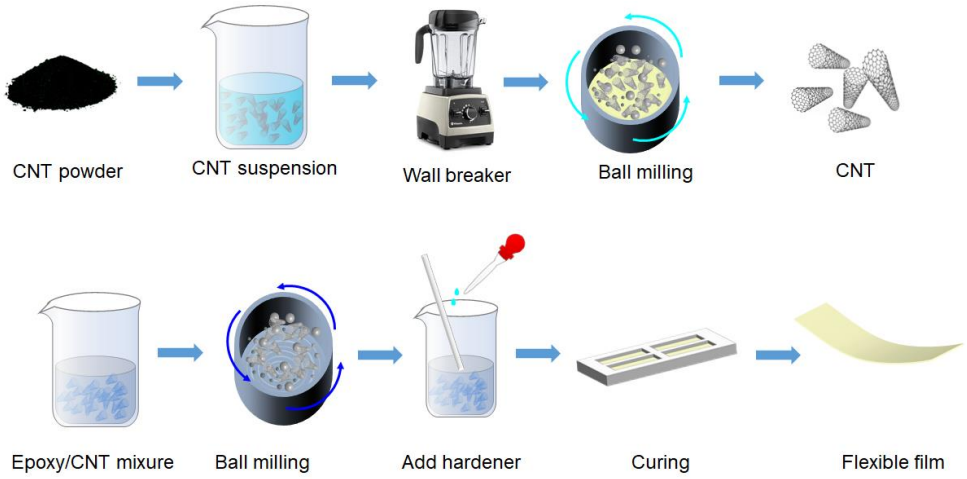

Figure 1. Illustration for the preparation of epoxy/CNT nanocomposites.

Epoxy/CNT nanocomposites: A predetermined weight of CNTs were dispersed in epoxy resin (E-51) using magnetic stirring for 30 min at 80 °C. It was then subjected to ball milling at 400 rpm for 12 h in a zirconia ball-milling container. In a glass container, epoxy/CNT mixtures were transferred to jeffamine-D2000 (hardener) at a weight ratio of 19:50 (E-51: D2000). The mixtures were then degassed for ten minutes at room temperature. The entire mixture was poured into a PTFE mold. We left the mold at 120 °C for 12 h. CNTs were present in different fractions (0.25, 0.5, and 1.0 vol%) in the prepared nanocomposites. Parallel to this, epoxy/CNT nanocomposites were produced by mechanical mixing in a similar manner. As a result of the apparent density of the CNTs (2.26 g/cm^3) and the matrix density (1.1 g/cm^3), the weight fractions (wt.%) were converted into volume percentages (vol%).

2.3. Characterization

The microstructure of CNTs and epoxy nanocomposites was studied by transmission electron microscopy (TEM) under a Philips CM200 microscope. TEM is operated at 200 KV acceleration voltage. Carbon nanotubes were suspended in organic solvent -methyl-2-pyrrolidone (NMP) at a concentration of 0.0004 wt.% and subjected to ultrasonic treatment at 30 °C for 30 min. The mixture is dripped onto a copper grid and dried in a 90 °C fan oven. Ultra-thin slices of 50 nm thickness were micro-cut from the prepared nanocomposites with a Leica Ultracut S-microtome diamond knife.

As part of the tensile test, dumbbell-shaped samples were prepared in accordance with ASTM D-638 (XIANGMIN, Shenzhen, China); the strain rate was set to 0.5 mm/min, and the tension machine was equipped with two 2 KN load components. The Young's modulus of epoxy samples was determined between 0.05% and 0.15% strain. We tested each fraction at least five times in order to determine its average and standard deviation in terms of tensile properties.

The thermal stability was determined by TA Q-50 (USA) curves at 20 °C/min from room temperature to 800 °C under N_2.

The electrical conductivity of the nanocomposites was measured with a Keisley 6517B high resistivity meter (Tektronix, Inc, Shanghai, China), resistivity model 8009. Samples with a thickness of 2 ± 0.5 mm and a diameter of 50 mm were tested at room temper-

ature. Three measurements were made to obtain the average thermal conductivity. An epoxy/CNT thin film sensor was measured with a FLUKE 2638A multimeter (Fluke Calibration, Beijing China) using a two-point method. During testing, two copper electrical contacts were placed on the film at a spacing of 30 mm using silver paint rings.

3. Result and Discussion

3.1. Analysis of Carbon Nanotube

Thermogravimetric analysis (TGA) was employed to investigate the thermal stability of carbon nanotubes (CNTs) under N_2 atmosphere, with heating ranging from 50 to 800 °C, as depicted in Figure 2a. The TGA results revealed that the CNTs did not exhibit any significant weight loss at 800 °C, indicating their high thermal stability. After, the as-received CNT product is unwound using the wall breaker and ball mill where the length of the CNTs will be reduced. Under the shear force of the action, the intertwined CNTs will separate from each other, resulting in a decrease in size. The transmission electron microscopy (TEM) image of CNTs dropped from an aqueous solution is presented in Figure 2b, revealing the individual existence of CNTs and confirming their well-dispersed and disentangled characteristics. The homogeneous dispersion of CNTs is crucial for the development of electrically conductive nanocomposites with high mechanical performance [35,36].

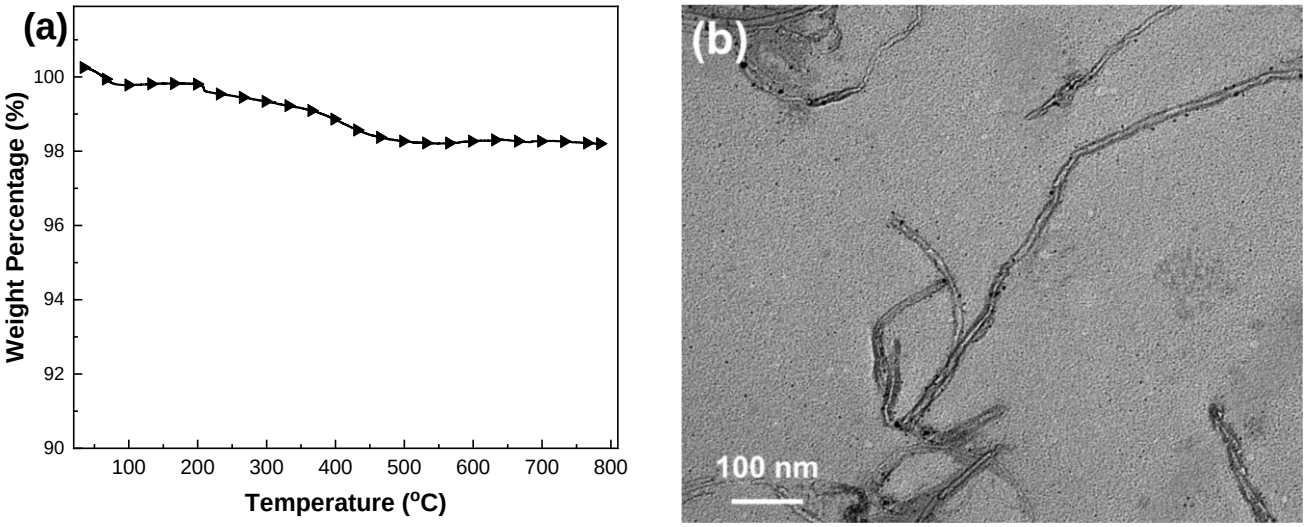

Figure 2. (**a**) TGA and (**b**) TEM of carbon nanotube (CNT).

3.2. Morphologies of the Nanocomposite

In order to investigate the dispersion of CNTs in the epoxy matrix, TEM images of epoxy/CNT nanocomposites with different preparation methods were obtained at a volume fraction of 0.50 and are presented in Figure 3. The mechanical mixing method resulted in obvious CNT agglomeration in the epoxy matrix, likely due to uneven dispersion caused by strong van der Waals interactions between the large number of CNTs in the matrix, as shown in Figure 3(a1). Selected areas were further magnified in Figure 3(a2), revealing entangled CNTs. In contrast, ball milling led to better CNT dispersion in the matrix, as seen in Figure 3(b1). The shear force during ball milling mildly damaged the CNT end-caps, leaving the ends open and transforming the long tubes into short fragments, as shown in Figure 3(b2). The disordered edges at the ends of the CNTs in Figure 3(b2) suggested that the ends were created after violently breaking the original CNTs, as opposed to the ordered ends observed in Figure 3(a2). The high aspect ratio of CNTs, which can reach up to 1000, enables them to form a global, rigid, and strong network inside the matrix, resisting applied loads and exhibiting high Young's moduli.

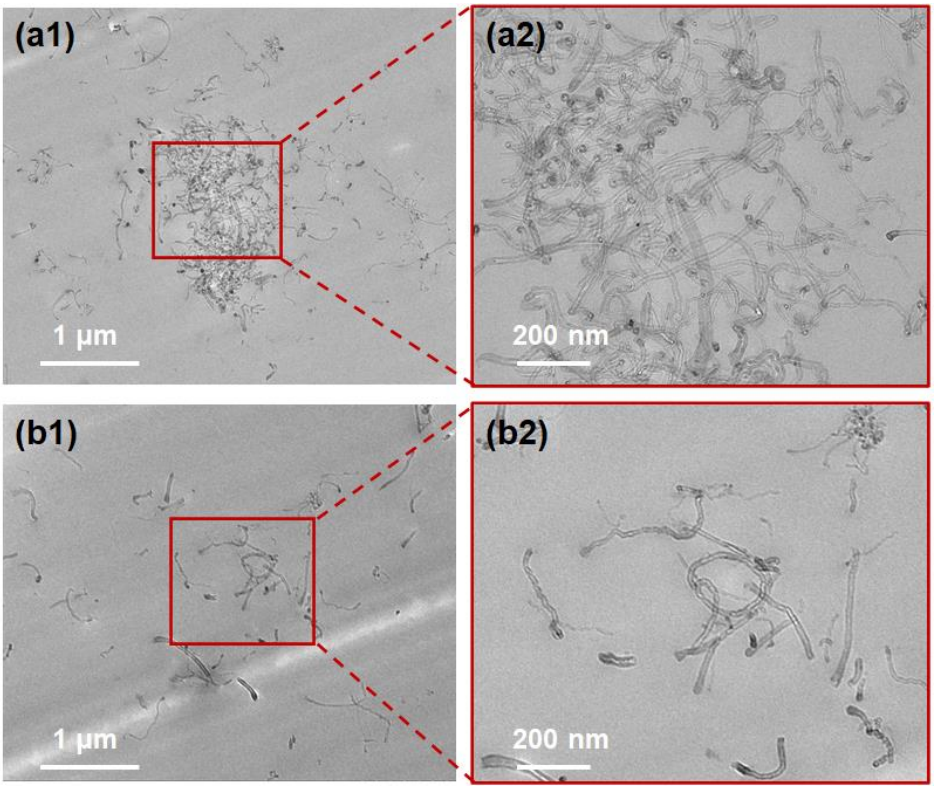

Figure 3. TEM images of epoxy/CNT nanocomposites with different preparation methods at 0.5 vol%: (**a1**,**a2**) mechanical mixing and (**b1**,**b2**) ball milling.

3.3. Mechanical Properties of the Nanocomposites

Mechanical properties are an essential evaluation index for polymers in various applications. However, the incorporation of carbon nanomaterials significantly alters the mechanical behavior of polymers. The mechanical properties of epoxy/CNT nanocomposites prepared by different methods was investigated, as presented in Figure 4. The incorporation of CNTs into the epoxy via ball milling resulted in a more substantial improvement than the mechanical mixing method.

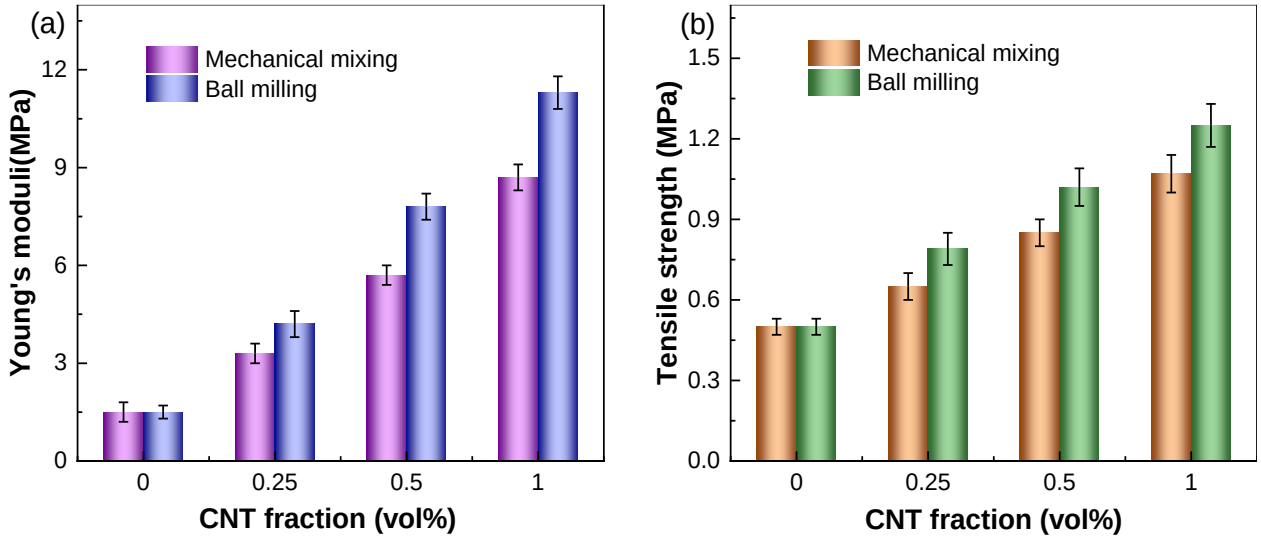

Figure 4. (**a**) Young's moduli and (**b**) tensile strength of epoxy/CNT nanocomposites with different preparation methods.

The Young's modulus and the tensile strength of the epoxy/CNT nanocomposites increased by 653% and 150%, respectively, upon the addition of 1.00 vol% CNTs through ball milling, which was higher than the values obtained for the mechanical mixing method, i.e., 480% and 114%. The greater improvement in the mechanical properties of the epoxy/CNT systems prepared by ball milling may be attributed to the superior dispersion of CNTs in the epoxy compared to the mechanical mixing process (see Figure 3). Ball milling mildly damaged the CNT end-caps, leaving the ends open and transforming the long tubes into short fragments, which achieved a relatively uniform dispersion of CNTs in the matrix in Figure 3. The well-dispersed CNTs in the matrix resulted in the formation of more uniform stress concentration centers in the matrix and reduced the failure strength of the samples prepared by mechanical mixing. Furthermore, due to the excellent physical and chemical properties of CNTs, stress can be effectively transferred from the matrix to the nano-filler, thereby improving the mechanical strength of the epoxy.

3.4. Thermal Stability

Thermogravimetric analysis (TGA) was carried out to assess the thermal stability of epoxy and epoxy/CNT nanocomposites under N_2 atmospheres. Epoxy/CNT nanocomposites possess a one-stage degradation process under N_2 in Figure 5a, exhibiting similar decomposition behaviors to neat epoxy, where the first stage is mainly due to the thermal degradation of epoxy chain networks. T_{onset} and T_{max} respectively refer to the temperatures where the 5% weight loss and the maximum weight loss rate occur. From Figure 5a,b, T_{onset} and T_{max} of epoxy/CNT nanocomposites are higher than a neat epoxy system, which is expected as the introduction of CNTs improves the thermal stability of epoxy. When compared to the epoxy/CNT prepared by the mechanical stirring (MS) method, the epoxy/CNT systems prepared by ball milling (BM) exhibit higher T_{onset} and T_{max}, which could be attributed to the fact that the relatively uniformly dispersion of CNTs in the matrix was improved by ball milling. The nanotubes of relatively uniform dispersion are more likely to form a three-dimensional thermal barrier in the matrix.

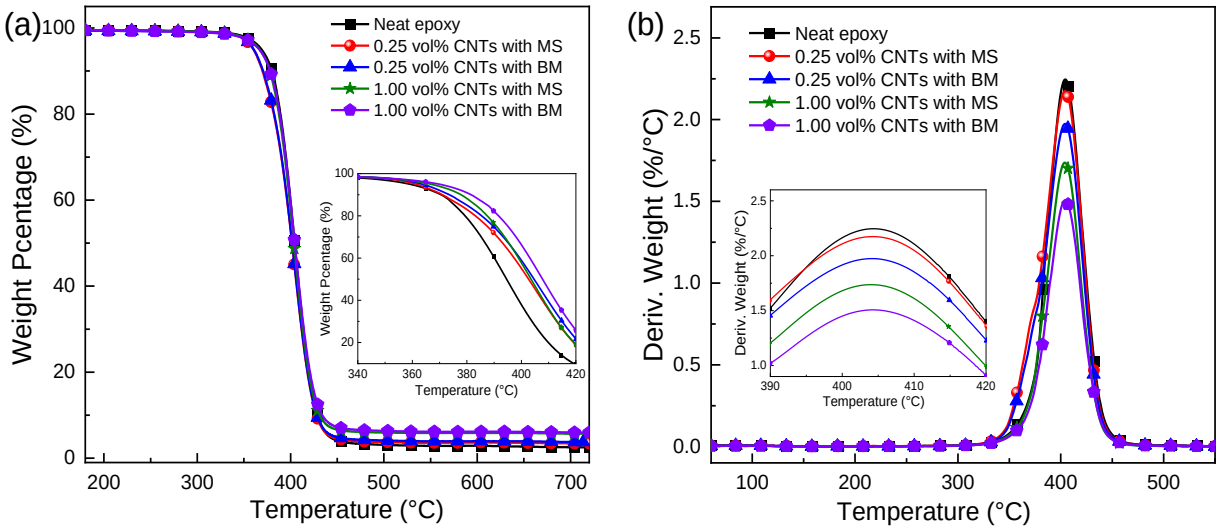

Figure 5. Epoxy and Epoxy/CNT nanocomposites: (**a**) TG curve and (**b**) DTG curve under N_2.

3.5. Electrical and Thermal Conductivity

Epoxy resin is an intrinsically non-conductive material with a conductivity of approximately 10^{-13} S/cm. However, there is a strong need for electrically conductive epoxy composites in the aerospace and electronics industries, primarily as materials that are electrically anti-static. To meet this demand, conductive nanofillers such as metal-based particles and carbon-based materials are added to the epoxy matrix to improve its electrical conductivity. The formation of electrically conductive paths is dependent not only on the

electrical conductivity of the nanofiller, but also on the geometry, volume fractions, and level of dispersion of the nanofiller within the matrix. A conductivity level of approximately ~10^{-8} S/cm is adequate for anti-static applications.

Figure 6 depicts the electrical conductivity of the epoxy/CNT nanocomposites with different preparation methods. It can be observed that the electrical conductivity of the neat epoxy is ~3×10^{-13} S/cm, which falls within the range (10^{-12}~10^{-14} S/cm) reported in previous studies on epoxy [37–39]. The addition of CNTs using both hand stirring and ball milling methods led to an increase in the electrical conductivity of the epoxy/CNT nanocomposites. As the volume fraction of CNTs increased, the inter-filler distance reduced, and at a certain threshold (percolation threshold), a network of conductive paths was formed by the fillers, thereby rendering the insulative nature of the epoxy ineffective. The experimental data were fitted into a power law equation to carry out further analysis:

$$\sigma_c = \sigma_f(\varphi - \varphi_t)^t \quad (1)$$

where σ_c is the nanocomposite conductivity, σ_f is the conductivity of the CNT, φ is the CNT vol%, φt is the percolation vol%, and t is the critical exponent. The epoxy/CNT systems that used the ball milling method showed a higher increment in electrical conductivity and a lower permeation threshold (0.67 vol%) compared to the mechanical mixing method (0.93 vol%). Furthermore, it is worth noting that the critical exponent t = 2.89 for the ball milling method is higher than the critical exponent t = 2.54 for the mechanical mixing method, indicative of a CNT filler network closer to the 3D type architecture through ball milling. These results suggest that ball milling can significantly improve the dispersion of CNTs in the epoxy matrix, facilitating electron migration and creating continuous and efficient conductive pathways. In summary, the high-energy ball milling process improved the dispersion of the CNTs in the matrix, resulting in enhanced mechanical, electrical, and functional properties.

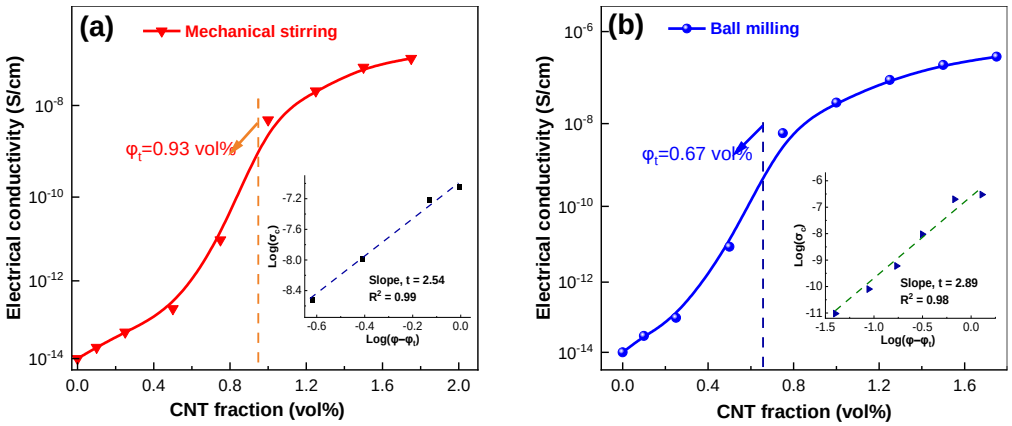

Figure 6. Electrical conductivity of epoxy/CNT nanocomposites with different preparation methods: (**a**) mechanical mixing and (**b**) ball milling.

3.6. Piezoresistive Performance

In this section, 1.0 vol% epoxy/CNT nanocomposite film was selected to examine its piezoresistive performance under various dynamic engineering applications. In the discussion below, the resistance change refers to $\Delta R = R - R_0$ and the relative resistance change is ΔR where R is the measured epoxy/CNT film resistance corresponding to the stimulating signal and R_0 is the film resistance at zero signal (zero strain for instance).

Sensitivity is one of the most critical parameters to characterize the performance of a strain sensor, which is reflected as the slope of a sensitivity graph. The gauge factor of a composite sensor can be described by a math function, in some cases, by taking the first derivative of the polynomial regression function of a sensitivity graph [40]. By conducting linear regression analysis for the testing data, a fitted function with R^2 = 0.95 for the

sensitivity graph in Figure 7a is found to be a two-order polynomial function, which can be used to obtain a gauge factor. The gauge factor is calculated as:

$$GF = \frac{d(\Delta R/R_0)}{d\varepsilon} \quad (2)$$

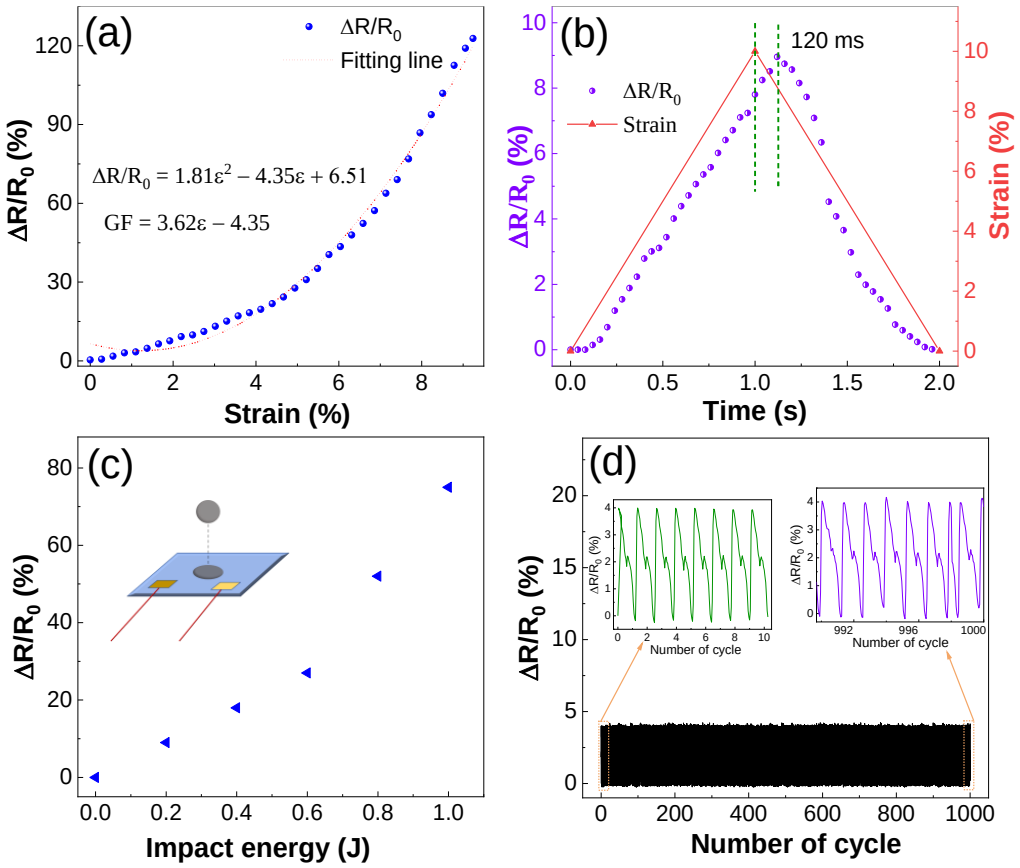

Figure 7. Electrical signal response of epoxy/CNT nanocomposites: (**a**) sensitivity, (**b**) response time, (**c**) impact energy, and (**d**) fatigue testing.

The gauge factor in Equation (2) is not a constant number but an algebraic function. The equation was then used to draw a graph of gauge factor vs. strain in Figure 7a. By substituting strain values of 0%–9.5%, the gauge factor was found to be in a range of 0–30 for the epoxy/CNT composite sensor. At very low strain, the resistance of the nanocomposite sensor changes little, and other environmental factors should cause fluctuations in the gauge factor.

In Figure 7b, the flexible film sensor could respond to external strain within 120 ms and recover to standby in 0.08 s. It is likely that its ultra-fast response-ability is related to the rapid recovery from the epoxy deformation, in addition to the performance of CNT materials.

Figure 7c depicts the resistance-impact energy response of the flexible film sensor. Different impact energies are simulated by controlling the falling height of a steel ball. The relative resistance increases linearly from 0 to 78% within an impact energy range of 0–1 J. This indicates that the epoxy/CNT flexible film may work as a multi-stimulus, high-sensitivity sensor for structural health monitoring.

High-mechanical durability is required for maintaining a stable input-output relationship in flexible sensors under long-term or cyclic loading. In Figure 7d, the flexible sensor was tested under repetitive cycles of 3% strain at 1 Hz. To further demonstrate the hysteresis characteristic of the flexible sensor, a typical loading-unloading cycle is inset in Figure 7d. As can be seen in the magnified view insets, there is no obvious degradation in

current amplitude during the whole process of loading/unloading test cycles. The excellent durability is attributed to the intrinsic stability of the CNT and the strong attachment between the CNT and the epoxy in the nanocomposite film.

3.7. Self-Sensing Performance

Self-sensing refers to the ability of a structural material to sense its own condition, such as strain, damage, and temperature [41–44]. One key advantage of this approach is the ability to monitor the entire volume of a component, in contrast to traditional strain gauges, which provide localized measurements. Structural materials possess intrinsic properties that can be leveraged to achieve self-sensing. Accurate detection and measurement of damage in structural components are critical, as they provide valuable information for maintenance and repair, particularly in the field of civil engineering [45–47].

Detecting and localizing damage in structural components is crucial for efficient maintenance and repair. To achieve this goal, a flexible sensor is placed on a horizontal table and a practical impact simulation is conducted. Figure 8a illustrates that the lower left corner and center parts were hit. The resistance change rate of the film sensor varies under external strain. Based on this principle, a strain contour cloud map can be generated to identify the damage location. The map also indicates the areas with higher force, displayed as red, and the regions with lower force, shown as blue.

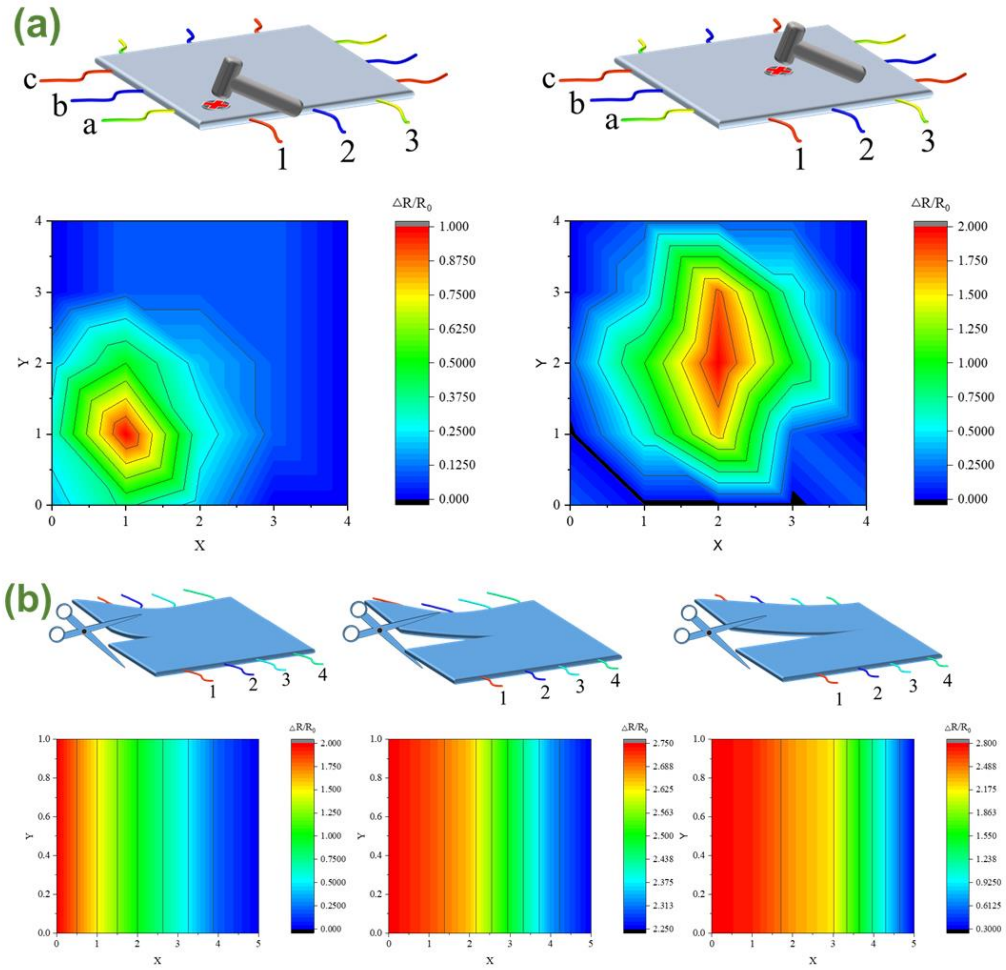

Figure 8. Self-sensing performance of epoxy/CNT nanocomposites: (**a**) knock and (**b**) crack.

The monitoring of crack propagation is a crucial aspect of structural health monitoring. For this purpose, a four-channel film sensor was employed to detect the location of the damage by comparing the electrical resistivity measurements from different sensors. The

sensor channels were selected to enable accurate identification of the damage location. To monitor the crack growth over time, scissors were used to successively cut the channel sensors 1–4, resulting in different electrical responses at different times in Figure 8b. It was observed that the resistance change rate of the cut part increased with the length of cutting. CNTs with relatively uniform dispersion tend to form three-dimensional interconnected network structures in the matrix, which can transfer stress and electrons more effectively. Therefore, the prepared epoxy/CNTs have high mechanical and electrical conductivity and self-sensing performance, which greatly broadens their application fields.

4. Conclusions

A cost-effective and environmentally friendly mechanochemical approach was utilized to synthesize high-performance epoxy nanocomposites with excellent mechanical and functional properties. The effect of various preparation methods on the mechanical properties of epoxy/CNT nanocomposites was investigated. Ball milling was found to significantly enhance the dispersion of CNTs within the epoxy matrix, leading to a 653% increase in Young's modulus and a 150% increase in tensile strength for epoxy/CNTs at 1.0 vol%, compared to the respective values of 480% and 114% for the mechanical mixing method. The electrical conductivity of the epoxy/CNT nanocomposites was also examined, revealing that ball milling resulted in a lower percolation threshold of 0.67 vol%, compared to 0.93 vol% for the mechanical mixing method. Moreover, the developed epoxy/CNT film sensor exhibited remarkable strain sensitivity under tensile strain and impact loading and demonstrated excellent self-sensing ability to damage evolution and position. This study presents a novel approach for developing highly functional epoxy nanocomposites with outstanding performance characteristics.

Author Contributions: Z.G.: Writing—original draft; Q.H.: Data curation; Methodology; J.L.: Supervision; K.Z.: Resources; Y.Y.: Data curation; Y.F.: Project administration; S.H.: Writing—review & editing; Supervision. All authors have read and agreed to the published version of the manuscript.

Funding: This research received no external funding.

Institutional Review Board Statement: Not applicable.

Informed Consent Statement: Not applicable.

Data Availability Statement: Not applicable.

Conflicts of Interest: The authors declare no conflict of interest.

References

1. Natarajan, K. Antibiofilm Activity of Epoxy/Ag-TiO_2 Polymer Nanocomposite Coatings against Staphylococcus Aureus and Escherichia Coli. *Coatings* **2015**, *5*, 95–114.
2. Serra, A.; Ramis, X.; Fernández-Francos, X. Epoxy Sol-Gel Hybrid Thermosets. *Coatings* **2016**, *6*, 8. [CrossRef]
3. Ibrahim, M.; Kannan, K.; Parangusan, H.; Eldeib, S.; Shehata, O.; Ismail, M.; Zarandah, R.; Sadasivuni, K.K. Enhanced Corrosion Protection of Epoxy/ZnO-NiO Nanocomposite Coatings on Steel. *Coatings* **2020**, *10*, 783. [CrossRef]
4. Kim, M.I.; Kim, S.; Kim, T.; Lee, D.K.; Seo, B.; Lim, C.-S. Mechanical and Thermal Properties of Epoxy Composites Containing Zirconium Oxide Impregnated Halloysite Nanotubes. *Coatings* **2017**, *7*, 231. [CrossRef]
5. Wang, N.; Gao, H.; Zhang, J.; Kang, P. Effect of Graphene Oxide/ZSM-5 Hybrid on Corrosion Resistance of Waterborne Epoxy Coating. *Coatings* **2018**, *8*, 179. [CrossRef]
6. Wu, Q.; Sundborg, H.; Andersson, R.L.; Peuvot, K.; Guex, L.; Nilsson, F.; Hedenqvist, M.S.; Olsson, R.T. Conductive biofoams of wheat gluten containing carbon nanotubes, carbon black or reduced graphene oxide. *RSC Adv.* **2017**, *7*, 18260–18269. [CrossRef]
7. Sam-Daliri, O.; Faller, L.-M.; Farahani, M.; Roshanghias, A.; Oberlercher, H.; Mitterer, T.; Araee, A.; Zangl, H. MWCNT–Epoxy Nanocomposite Sensors for Structural Health Monitoring. *Electronics* **2018**, *7*, 143. [CrossRef]
8. Yang, S.; Zhu, S.; Hong, R. Graphene Oxide/Polyaniline Nanocomposites Used in Anticorrosive Coatings for Environmental Protection. *Coatings* **2020**, *10*, 1215. [CrossRef]
9. Yan, X.; Qian, X.; Chang, Y. Preparation and Characterization of Urea Formaldehyde @ Epoxy Resin Microcapsule on Waterborne Wood Coatings. *Coatings* **2019**, *9*, 475. [CrossRef]
10. Han, S.; Meng, Q.; Qiu, Z.; Osman, A.; Cai, R.; Yu, Y.; Liu, T.; Araby, S. Mechanical, toughness and thermal properties of 2D material-reinforced epoxy composites. *Polymer* **2019**, *184*, 121884. [CrossRef]

11. Han, S.; Wang, P.; Zhou, Y.; Meng, Q.; Aakyiir, M.; Ma, J. Flexible, mechanically robust, multifunctional and sustainable cellulose/graphene nanocomposite films for wearable human-motion monitoring. *Compos. Sci. Technol.* **2022**, *230*, 109451. [CrossRef]
12. Zhang, J.; Mi, X.; Chen, S.; Xu, Z.; Zhang, D.; Miao, M.; Wang, J. A bio-based hyperbranched flame retardant for epoxy resins. *Chem. Eng. J.* **2020**, *381*, 122719. [CrossRef]
13. Yu, B.; Shi, Y.; Yuan, B.; Qiu, S.; Xing, W.; Hu, W.; Song, L.; Lo, S.; Hu, Y. Enhanced thermal and flame retardant properties of flame-retardant-wrapped graphene/epoxy resin nanocomposites. *J. Mater. Chem. A* **2015**, *3*, 8034–8044. [CrossRef]
14. Zhou, K.; Gao, R.; Qian, X. Self-assembly of exfoliated molybdenum disulfide (MoS_2) nanosheets and layered double hydroxide (LDH): Towards reducing fire hazards of epoxy. *J. Hazard. Mater.* **2017**, *338*, 343–355. [CrossRef] [PubMed]
15. Han, S.; Meng, Q.; Pan, X.; Liu, T.; Zhang, S.; Wang, Y.; Haridy, S.; Araby, S. Synergistic effect of graphene and carbon nanotube on lap shear strength and electrical conductivity of epoxy adhesives. *J. Appl. Polym. Sci.* **2019**, *136*, 48056. [CrossRef]
16. Han, S.; Chand, A.; Araby, S.; Cai, R.; Chen, S.; Kang, H.; Cheng, R.; Meng, Q. Thermally and electrically conductive multifunctional sensor based on epoxy/graphene composite. *Nanotechnology* **2020**, *31*, 075702. [CrossRef] [PubMed]
17. Han, S.; Meng, Q.; Chand, A.; Wang, S.; Li, X.; Kang, H.; Liu, T. A comparative study of two graphene based elastomeric composite sensors. *Polym. Test.* **2019**, *80*, 106106. [CrossRef]
18. Meng, Q.; Liu, D.; Zhou, Y.; Cai, R.; Feng, Y.; Hu, Z.; Han, S. Durable, highly sensitive conductive elastomeric nanocomposite films containing various graphene nanoplatelets and their derivatives. *Polym. Adv. Technol.* **2023**, *34*, 1170–1181. [CrossRef]
19. Hicks, J.F.; Seok-Shon, Y.; Murray, R.W. Layer-by-Layer Growth of Polymer/Nanoparticle Films Containing Monolayer-Protected Gold Clusters. *Langmuir* **2002**, *18*, 2288–2294. [CrossRef]
20. Meng, Q.; Liu, Z.; Han, S.; Xu, L.; Araby, S.; Cai, R.; Zhao, Y.; Lu, S.; Liu, T. A facile approach to fabricate highly sensitive, flexible strain sensor based on elastomeric/graphene platelet composite film. *J. Mater. Sci.* **2019**, *54*, 10856–10870. [CrossRef]
21. Meng, Q.; Liu, Z.; Cai, R.; Han, S.; Lu, S.; Liu, T. Non-oxidized graphene/elastomer composite films for wearable strain and pressure sensors with ultra-high flexibility and sensitivity. *Polym. Adv. Technol.* **2020**, *31*, 214–225. [CrossRef]
22. Meng, Q.; Kenelak, V.; Chand, A.; Kang, H.; Han, S.; Liu, T. A highly flexible, electrically conductive, and mechanically robust graphene/epoxy composite film for its self-damage detection. *J Appl Polym Sci.* **2020**, *137*, 48991. [CrossRef]
23. Capezza, A.; Andersson, R.L.; Ström, V.; Wu, Q.; Sacchi, B.; Farris, S.; Hedenqvist, M.S.; Olsson, R.T. Preparation and Comparison of Reduced Graphene Oxide and Carbon Nanotubes as Fillers in Conductive Natural Rubber for Flexible Electronics. *ACS Omega* **2019**, *4*, 3458–3468. [CrossRef] [PubMed]
24. Zou, B.; Qiu, S.; Ren, X.; Zhou, Y.; Zhou, F.; Xu, Z.; Zhao, Z.; Song, L.; Hu, Y.; Gong, X. Combination of black phosphorus nanosheets and MCNTs via phosphoruscarbon bonds for reducing the flammability of air stable epoxy resin nanocomposites. *J. Hazard Mater.* **2020**, *383*, 121069. [CrossRef]
25. Breitwieser, A.; Siedlaczek, P.; Lichtenegger, H.; Sleytr, U.B.; Pum, D. S-Layer Protein Coated Carbon Nanotubes. *Coatings* **2019**, *9*, 492. [CrossRef]
26. Kim, S.; Jeong, H.; Choi, S.-H.; Park, J.-T. Electrical Conductivity Measurement of Transparent Conductive Films Based on Carbon Nanoparticles. *Coatings* **2019**, *9*, 499. [CrossRef]
27. Ma, H.; Zhao, L.; Liu, J.; Wang, J.; Xu, J. Functionalizing carbon nanotubes by grafting cyclotriphosphazene derivative to improve both mechanical strength and flame retardancy. *Polym. Compos.* **2014**, *35*, 2187–2193. [CrossRef]
28. Meng, Q.; Jin, J.; Wang, R.; Kuan, H.C.; Ma, J.; Kawashima, N.; Michelmore, A.; Zhu, S.; Wang, C.H. Processable 3-nm thick graphene platelets of high electrical conductivity and their epoxy composites. *Nanotechnology* **2014**, *25*, 125707. [CrossRef]
29. Ma, J.; Meng, Q.; Zaman, I.; Zhu, S.; Michelmore, A.; Kawashima, N.; Wang, C.H.; Kuan, H.C. Development of polymer composites using modified, high-structural integrity graphene platelets. *Compos. Sci. Technol.* **2014**, *91*, 82–90. [CrossRef]
30. Zaman, I.; Kuan, H.C.; Dai, J.; Kawashima, N.; Michelmore, A.; Sovi, A.; Dong, S.; Luong, L.; Ma, J. From carbon nanotubes and silicate layers to graphene platelets for polymer nanocomposites. *Nanoscale* **2012**, *4*, 4578–4586. [CrossRef]
31. Meng, Q.; Han, S.; Liu, T.; Ma, J.; Ji, S.; Dai, J.; Kang, H.; Ma, J. Noncovalent Modification of Boron Nitrite Nanosheets for Thermally Conductive, Mechanically Resilient Epoxy Nanocomposites. *Ind. Eng. Chem. Res.* **2020**, *59*, 20701–20710. [CrossRef]
32. Meng, Q.; Song, X.; Han, S.; Abbassi, F.; Zhou, Z.; Wu, B.; Wang, X.; Araby, S. Mechanical and functional properties of polyamide/graphene nanocomposite prepared by chemicals free-approach and selective laser sintering. *Compos. Commun.* **2022**, *36*, 101396. [CrossRef]
33. Deng, S.; Zhang, J.; Ye, L. Halloysite-epoxy nanocomposites with improved particle dispersion through ball mill homogenisation and chemical treatments. *Compos. Sci. Technol.* **2009**, *69*, 2497–2505. [CrossRef]
34. Huang, H.-C.; Huang, S.-P.; Hsieh, T.-E.; Chen, C.-H. Characterizations of UV-curable montmorillonite/epoxy nanocomposites prepared by a hybrid of chemical dispersion and planetary mechanical milling process. *J. Appl. Polym. Sci.* **2012**, *123*, 3199–3207. [CrossRef]
35. Han, S.; Meng, Q.; Araby, S.; Liu, T.; Demiral, M. Mechanical and electrical properties of graphene and carbon nanotube reinforced epoxy adhesives: Experimental and numerical analysis. *Compos. Part A Appl. Sci. Manuf.* **2019**, *120*, 116–126. [CrossRef]
36. Sun, K.; Duan, W.X.; Lei, Y.H.; Wang, Z.X.; Tian, J.H.; Yang, P.T.; He, Q.F.; Chen, M.; Wu, H.K.; Zhang, Z.; et al. Flexible multi-walled carbon nanotubes/polyvinylidene fluoride membranous composites with weakly negative permittivity and low frequency dispersion. *Compos. Part A Appl. Sci. Manuf.* **2022**, *156*, 106854. [CrossRef]

37. Meng, Q.; Han, S.; Araby, S.; Zhao, Y.; Liu, Z.; Lu, S. Mechanically robust, electrically and thermally conductive graphene-based epoxy adhesives. *J. Adhes. Sci. Technol.* **2019**, *33*, 1337–1356. [CrossRef]
38. Meng, Q.; Zhao, Y.; Liu, Z.; Han, S.; Lu, S.; Liu, T. Flexible strain sensors based on epoxy/graphene composite film with long molecular weight curing agents. *J. Appl. Polym. Sci.* **2019**, *136*, 47906. [CrossRef]
39. Wang, S.; Cai, R.; Xue, H.; Liu, T.; Han, S.; Zhou, Z.; Hu, Z.; Meng, Q. Development of high thermally conductive and electrically insulated epoxy nanocomposites with high mechanical performance. *Polym. Compos.* **2021**, *42*, 4217–4226. [CrossRef]
40. Han, S.; Zhang, X.; Wang, P.; Dai, J.; Guo, G.; Meng, Q.; Ma, J. Mechanically robust, highly sensitive and superior cycling performance nanocomposite strain sensors using 3-nm thick graphene platelets. *Polym. Test.* **2021**, *98*, 107178. [CrossRef]
41. Han, S.; Meng, Q.; Xing, K.; Araby, S.; Yu, Y.; Mouritz, A.; Ma, J. Epoxy/graphene film for lifecycle self-sensing and multifunctional applications. *Compos. Sci. Technol.* **2020**, *198*, 108312. [CrossRef]
42. Bareia, T.; Pollak, S.; Eldar, A. Self-sensing in Bacillus subtilis quorum-sensing systems. *Nat. Microbiol.* **2018**, *3*, 83–89. [CrossRef] [PubMed]
43. Lo, C.-Y.; Zhao, Y.; Kim, C.; Alsaid, Y.; Khodambashi, R.; Peet, M.; Fisher, R.; Marvi, H.; Berman, S.; Aukes, D.; et al. Highly stretchable self-sensing actuator based on conductive photothermally-responsive hydrogel. *Mater. Today* **2021**, *50*, 35–43. [CrossRef]
44. Dong, L.; Ren, M.; Wang, Y.; Qiao, J.; Wu, Y.; He, J.; Wei, X.; Di, J.; Li, Q. Self-sensing coaxial muscle fibers with bi-lengthwise actuation. *Mater. Horiz.* **2021**, *8*, 2541–2552. [CrossRef] [PubMed]
45. Yoo, S.J.; Kim, S.; Cho, K.-H.; Ahn, H.-J. Data-Driven Self-sensing Technique for Active Magnetic Bearing. *Int. J. Precis. Eng. Manuf.* **2021**, *22*, 1031–1038. [CrossRef]
46. Birgin, H.B.; D'Alessandro, A.; Corradini, A.; Laflamme, S.; Ubertini, F. Self-sensing asphalt composite with carbon microfibers for smart weigh-in-motion. *Mater. Struct.* **2022**, *55*, 138. [CrossRef]
47. Gong, Z.; Han, L.; An, Z.; Yang, L.; Ding, S.; Xiang, Y. Empowering smart buildings with self-sensing concrete for structural health monitoring. In Proceedings of the ACM SIGCOMM 2022 Conference, Amsterdam, The Netherlands, 22–26 August 2022; pp. 560–575.